Molecular Therapy
Oncolytics
Original Article

NAD+ depletion enhances reovirus-induced oncolysis in multiple myeloma

Barry E. Kennedy,[1] Michael Giacomantonio,[1] J. Patrick Murphy,[1,2] Samuel Cutler,[1] Maryanne Sadek,[1] Prathyusha Konda,[3] Joao A. Paulo,[4] Gopal P. Pathak,[1] Saskia H.J. Renkens,[1] Stacy Grieve,[5] Jonathan Pol,[6,7,8,9,10,11] Steven P. Gygi,[4] Christopher Richardson,[3,12] Daniel Gaston,[1,13,14] Anthony Reiman,[5,15,16] Guido Kroemer,[13,14,17,18,19,20] Manal O. Elnenaei,[1,21] and Shashi A. Gujar[1,2,3,21,22]

[1]Department of Pathology, Dalhousie University, Rm. 11J Sir Charles Tupper Medical Building, 5850 College Street, Halifax, NS B3H 1X5, Canada; [2]Department of Biology, University of Prince Edward Island, Charlottetown, PEI C1A 4P3, Canada; [3]Department of Microbiology and Immunology, Dalhousie University, Halifax, NS B3H 1X5, Canada; [4]Department of Cell Biology, Harvard Medical School, Boston, MA 02115, USA; [5]Department of Biology, University of New Brunswick, Saint John E2L 4L2, Canada; [6]Gustave Roussy Comprehensive Cancer Institute, Villejuif 94800, France; [7]Metabolomics and Cell Biology Platforms, Gustave Roussy Cancer Campus, Villejuif 94800, France; [8]INSERM, U1138, Paris 75006, France; [9]Équipe 11 labellisée par la Ligue Nationale Contre le Cancer, Centre de Recherche des Cordeliers, Paris 75006, France; [10]Université de Paris, Paris 75006, France; [11]Sorbonne Université, Paris 75006, France; [12]Department of Pediatrics, Dalhousie University, Halifax, NS B3H 1X5, Canada; [13]Department of Pathology and Laboratory Medicine, Nova Scotia Health Authority (NSHA), Halifax, NS B3H 1V8, Canada; [14]Department of Pathology, Dalhousie University, Halifax, NS B3H 1V8, Canada; [15]Department of Oncology, University of New Brunswick, Saint John E2L 4L2, Canada; [16]Department of Medicine, Dalhousie University, Halifax, NS B3H 1X5, Canada; [17]Institut Universitaire de France, Paris 75005, France; [18]Pôle de Biologie, Hôpital Européen Georges Pompidou, AP-HP, Paris 75015, France; [19]Suzhou Institute for Systems Medicine, Chinese Academy of Medical Sciences, Suzhou 215163, China; [20]Karolinska Institute, Department of Women's and Children's Health, Karolinska University Hospital, Stockholm 171 76, Sweden; [21]Beatrice Hunter Cancer Research Institute, Halifax, NS B3H 4R2, Canada

Cancer cell energy metabolism plays an important role in dictating the efficacy of oncolysis by oncolytic viruses. To understand the role of multiple myeloma metabolism in reovirus oncolysis, we performed semi-targeted mass spectrometry-based metabolomics on 12 multiple myeloma cell lines and revealed a negative correlation between NAD+ levels and susceptibility to oncolysis. Likewise, a negative correlation was observed between the activity of the rate-limiting NAD+ synthesis enzyme NAMPT and oncolysis. Indeed, depletion of NAD+ levels by pharmacological inhibition of NAMPT using FK866 sensitized several myeloma cell lines to reovirus-induced killing. The myelomas that were most sensitive to this combination therapy expressed a functional p53 and had a metabolic and transcriptomic profile favoring mitochondrial metabolism over glycolysis, with the highest synergistic effect in KMS12 cells. Mechanistically, U-^{13}C-labeled glucose flux, extracellular flux analysis, multiplex proteomics, and cell death assays revealed that the reovirus + FK866 combination caused mitochondrial dysfunction and energy depletion, leading to enhanced autophagic cell death in KMS12 cells. Finally, the combination of reovirus and NAD+ depletion achieved greater antitumor effects in KMS12 tumors *in vivo* and patient-derived CD138+ multiple myeloma cells. These findings identify NAD+ depletion as a potential combinatorial strategy to enhance the efficacy of oncolytic virus-based therapies in multiple myeloma.

INTRODUCTION

Multiple myeloma (MM) is a plasma cell neoplasm that accounts for approximately 10% of all hematologic malignancies.[1] MM has a 5-year survival rate of under 50% and is invariably fatal, with current therapies failing to overcome refractory disease or prevent recurrence.[2] Thus, there is a desperate need for new and efficacious MM therapeutic options. Oncolytic viruses (OVs) have shown promising results in a wide range of cancers including MM and represent a novel anticancer therapeutic avenue.[3,4] OVs act by preferentially targeting and killing cancer cells through both direct lysis and induction of potent antitumor immune responses while leaving normal cells unharmed.[5] One OV under investigation as an anti-MM therapy is reovirus, a naturally occurring dsRNA virus that is benign in humans.[6] Several studies have demonstrated that reovirus has the potential to kill MM cells through apoptosis or autophagy.[7,8] However, in a Phase 1 clinical trial performed on MM patients (NCT01533194[9]), the anticipated oncolysis was less than optimal. Thus, approaches enhancing the oncolytic capacity of reovirus, for instance by combination therapies,[10,11] are much needed.

Metabolic reprogramming can increase the susceptibility of cancer cells to OV-driven oncolysis.[12] Viruses hijack host cell metabolism to support their own growth. Exploiting this strategy, metabolic reprogramming has been used to enhance viral replication and

Received 10 September 2021; accepted 17 February 2022;
https://doi.org/10.1016/j.omto.2022.02.017.

[22]Lead contact

Correspondence: Shashi Gujar, Departments of Pathology, Microbiology & Immunology, Dalhousie University, Rm. 11J Sir Charles Tupper Medical Building, 5850 College Street, Halifax, NS B3H 1X5, Canada.
E-mail: shashi.gujar@dal.ca

oncolysis.[12,13] Recently, we found that an infection-induced block of pyruvate flux into mitochondria via inhibitory phosphorylation of pyruvate dehydrogenase (PDH), protected breast cancer cells from reovirus-induced oncolysis.[14] Consequently, pharmacologic or genetic inhibition of PDH kinases enhanced reovirus-induced oncolysis in breast cancer cells.[14] Whether MM harbors such therapeutically exploitable metabolic vulnerabilities in the context of OV therapies is unknown.[15]

Here, we observed that reovirus-induced oncolysis was negatively correlated with both nicotinamide adenine dinucleotide (NAD+) levels and activity of nicotinamide phosphoribosyl transferase (NAMPT; the rate-limiting enzyme within the NAD+ salvage pathway). Pharmacological inhibition of NAMPT with FK866 enhanced reovirus-induced oncolysis in several MM lines that especially expressed functional p53. Mechanistically, the combination of reovirus + FK866 lowered glucose flux into the tricarboxylic acid (TCA) cycle, thus leading to enhanced autophagy and oncolysis. Most importantly, following reovirus + FK866 combination therapy, patient-derived CD138+ MM cells underwent enhanced oncolysis, and mice xenografted with MM tumors showed prolonged survival compared with monotherapies. These results identify reovirus coupled with NAD+ synthesis inhibition as a novel combinatorial therapeutic strategy against MM.

RESULTS

Sensitivity of MM cells to OV oncolysis negatively correlates with NAD+ levels

Recently, we showed that metabolic reprogramming of cancer cells can enhance the oncolytic ability of OV.[14] To expand our understanding of the role of metabolism in reovirus-driven oncolysis of MM, we performed semi-targeted mass spectrometry-based metabolomics on a panel of 12 MM cell lines prior to infection and at a pre-lethal time point of 24 h post-infection (h.p.i.). This elucidated both basal (relative to the average of all cell lines) and reovirus-induced MM metabolic signatures of all cell lines (Figures S1A and S1B). Next, we determined the sensitivity to reovirus of the 12 MM cell lines as measured by cytotoxicity 72 h.p.i (Figure 1A). To identify metabolites that might contribute to reovirus-induced oncolysis, we correlated oncolysis with either reovirus-induced metabolic changes or basal metabolite levels in all cell lines (Figures 1B and S1C). One of the most negatively correlated metabolites with oncolysis was NAD+ (both at basal levels and after reovirus infection; Figures 1C and 1D). Supporting a role for NAD+, basal levels of the NAD+ -associated metabolites, glutathione (both reduced and oxidized) and glutamate negatively correlated with reovirus-induced cytotoxicity (Figures S1D–S1F).[16,17] Furthermore, basal expression levels of several NAD+-consuming enzymes (e.g., *SIRT6*), dehydrogenases (e.g., *NDUFS7*), or enzymes essential for maintaining NAD+ homeostasis (e.g., *GOT1*)[18] positively correlated with oncolysis, although other NAD+ -related enzymes, including NAD+ kinase (*NADK*), negatively correlated with oncolysis (Figures 1E–1G, S1G, and S1H).[19] Importantly, all but one cell line were highly infected (>45%, exception MOLP8) at 24 h.p.i (Figure S1I), and the percentage of infected cells did not correlate with either oncolysis or NAD+ levels (Figures S1J–S1L), ruling out differential infection rates as an explanation for varying sensitivities. Together, these results suggest that reovirus oncolysis is determined by factors downstream of infection and at least in part are driven by NAD+ -related pathways in MM.

Inhibition of NAMPT enhances reovirus oncolysis in MM cell lines that express functional p53 and favor mitochondrial metabolism

In most cancers including MM, NAD+ is mainly synthesized through the NAD+ salvage pathway.[20] In line with a prior report[21] we found that, of 1,019 cell lines across 36 different cancers in the cancer cell line encyclopedia (CCLE), MM cell lines had the second highest average mRNA expression of *NAMPT*, the rate-limiting enzyme of the NAD+ salvage pathway (Figure S2A). Complementing these data, MM cells have a much higher dependency on *NAMPT* for survival than other cancers according to the CERES CRISPR-Cas9 essentiality screen (Figure S2B).[22] To investigate the role of the NAD+ salvage pathway in reovirus-induced cytotoxicity, we first measured NAMPT protein levels in the context of reovirus infection. In accord with expression data, basal or reovirus-induced protein levels of NAMPT did not correlate with oncolysis (Figures S2C–S2F). However, as protein levels may not correlate with enzyme activity,[23] we measured the absolute log 2-fold change of NAD+ after treatment with a specific NAMPT inhibitor, FK866,[24] to determine NAMPT activity. In keeping with a contribution of NAD+ to oncolysis in MM, NAMPT activity negatively correlated with reovirus-induced cytotoxicity (Figures 2A, S2G, and S2H).

To test whether inhibition of NAMPT affects the sensitivity of MM cells to reovirus, we investigated oncolysis following the combination of FK866 reovirus. First, we measured FK866-induced cytotoxicity and found a range of sensitivities, consistent with published literature,[21] that positively correlated with reovirus-induced oncolysis (Figures S2I and S2J). To confirm the specificity of FK866, nicotinamide mononucleotide (NMN, the product of NAMPT enzymatic reaction and precursor to NAD+) was used to rescue cells from the effects of NAMPT inhibition. NMN supplementation recapitulated NAD+ levels in FK866-treated cells to those of untreated counterparts in all cell lines (Figures S2G–S2I). Next, by combining FK866 + reovirus, we were able to determine the role of NAD+ in reovirus-induced oncolysis. The responses to FK866 and reovirus were cell dependent: KMS11 and RPMI8226 were relatively resistant to both treatments, whereas 5TGM1, MOLP8, JJN3, KMS27, and MM1R were more sensitive to FK866 and showed no synergistic effect when combined with reovirus. KMM1 and U226 were more sensitive to reovirus and showed no synergistic effect when combined with FK866 (Figures 2B, 2C, and S3A). Finally, reovirus-mediated oncolysis was significantly enhanced by FK866 treatment in three cell lines: IM9, KMS12, and MM1S (Figures 2B, 2C, and S3A). In all cases, FK866-induced cell death was rescued by addition of NMN.

Previous studies of other cancers have reported that optimal sensitivity to FK866 and reovirus monotherapies require a specific gene

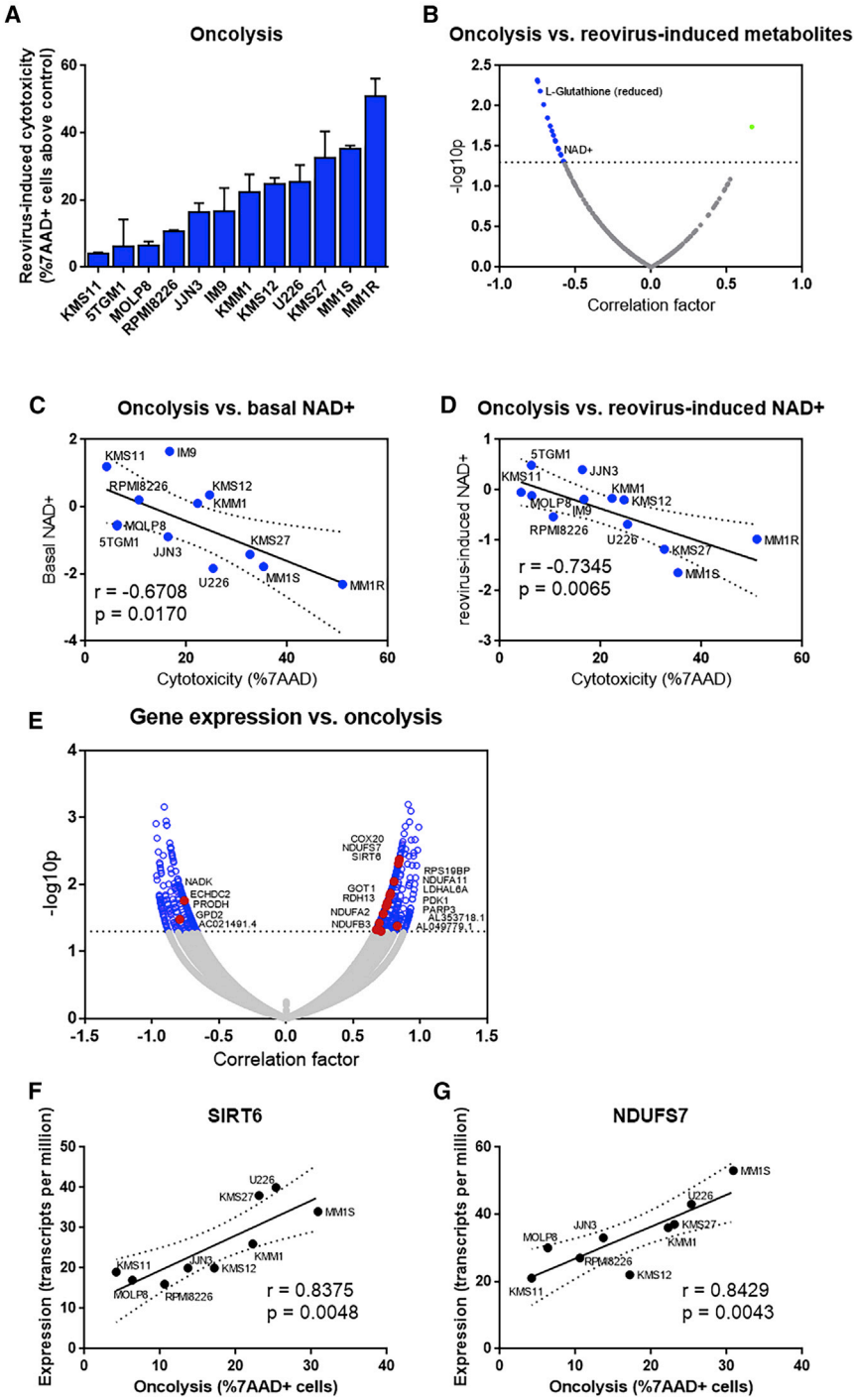

Figure 1. Basal and reovirus-induced NAD+ levels negatively correlate with reovirus oncolysis

(A) Percentage of cell death in MM cells caused by reovirus (MOI 10), 72 h.p.i. Data are means ± standard deviation from five independent experiments each performed in triplicates. (B) The correlation factor and –log10 probability of reovirus-induced changes in metabolites 24 h.p.i. versus percent oncolysis 72 h.p.i. in all MM cells. (C and D) Comparison of the respective susceptibility to reovirus oncolysis with the basal (C; log 2-fold compared with average of all cells) and reovirus-induced (D; log 2-fold compared with non-infected) NAD+ levels in MM cells. (E) The correlation factor and –log10 probability of gene expression (data from CCLE[16]) and percent cell death by reovirus in MM cells. Blue circles represent proteins that significantly correlate with oncolysis; red dots represent proteins that are involved in NAD+ metabolism. (F and G) Examples of the genes that correlate with oncolysis.

expression profile.[25–28] To better understand why certain cell lines were sensitive to combination therapy, we investigated global basal gene expression and mutational status of two genes known to play a role in monotherapy efficacy, the tumor suppressor *TP53* and the proto-oncogene *KRAS*.[25–28] In line with the literature for monotherapies, cell lines that are most sensitive to combination therapy (KMS27, MOLP8, IM9, KMS12, and MM1S) expressed wild-type or partially functional *TP53*, and in most cases, a wild-type *KRAS* (IM9 and KMS12, exception MM1S).[25–31] Conversely, cell lines that were most resistant contained loss-of-function or gain-of-(oncogenic)-function mutations in *TP53* (KMS11, RPMI8226, KMM1, U226, and JJN3) and gain-of-function mutations in *KRAS* (RPMI8226 and KMM1) (Figure 2C and Table S1).[25–29,31] In support of mutation analysis, basal expression levels of *TP53* and p53 stabilizer *MDM4*[32] positively correlated with sensitivity to combination therapy, whereas levels of *KRAS* negatively correlated with the combination-induced cytotoxicity (Figures 2D, 2E, S3B, and S3C). Functional p53 and mutated KRAS are known to have counteractive effects on several pathways including metabolism; p53 favors oxidative phosphorylation, and mutated KRAS favors aerobic glycolysis.[33,34] Indeed, p53-repressed glycolytic enzymes *PFKP* and *PFKM* negatively correlated with sensitivity to combination therapy, whereas the electron transport chain subunit succinate dehydrogenase cytochrome *b*560, positively correlated with sensitivity to combination therapy (Figures 2F, 2G, and S3D).[35,36] These data suggest FK866 + reovirus combination therapy requires MM to express functional p53 and wild-type KRAS and to have a metabolic profile that favors oxidative phosphorylation over glycolysis for optimal efficacy.

To explore the role of metabolism in combination therapy, we completed semi-targeted metabolomics analysis on all cell lines pre-

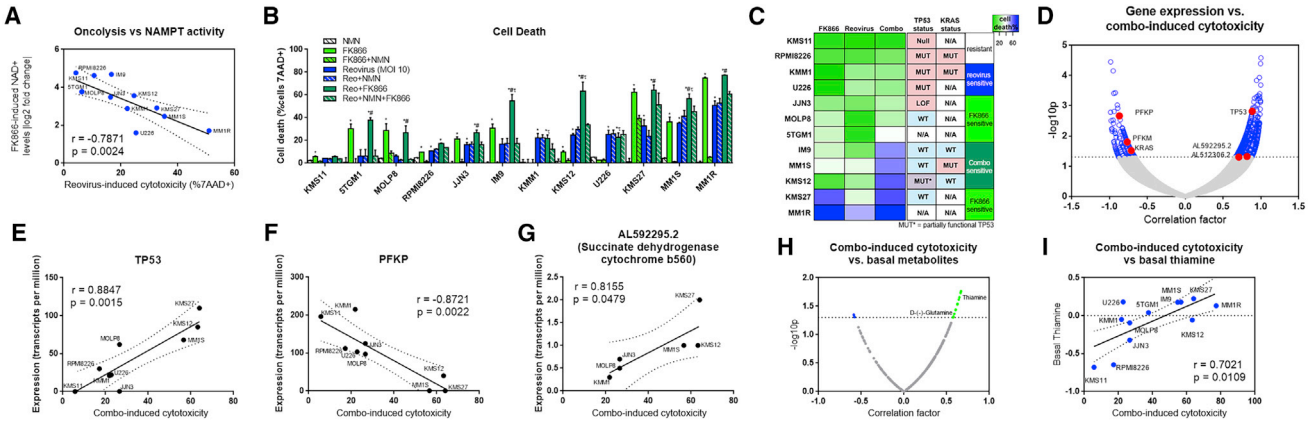

Figure 2. Inhibition of NAMPT enhances reovirus oncolysis in MM cell lines

(A) Correlation between NAMPT activity and reovirus oncolysis. (B) Percent cell death 72 h after reovirus infection, FK866 treatment, and/or NMN addition. Cell lines are shown in the order of their sensitivity to reovirus. Data are means ± standard deviation from five independent experiments in triplicates. *p < 0.05 versus NT, #p < 0.05 versus Reo, τp < 0.05 versus FK866. (C) Heatmap summarizing cell death and mutation status of *TP53* and *KRAS*. Cell lines are shown in the order of their sensitivity to combination therapy (combo). MUT, mutation; WT, wild type; LOE, loss of expression; *mutation (C)1010G > T maintains partial function; N/A, data unavailable; see Table S1 for more details. (D) The correlation factor and –log10 probability of gene expression (data from CCLE[16]) and percent cell death by reovirus + FK866 in MM cells. Blue circles represent proteins that significantly correlate with combination-induced oncolysis; red dots represent genes of interest. (E–G) Examples of the genes that correlate with combination-induced oncolysis. (H and I) The correlation factor and –log10 probability of basal metabolic levels (H) compared with percent cell death by combination treatment in all MM cells, with thiamine used as a representative metabolite (I).

and post-treatment with reovirus + FK866. Basal levels of thiamine (a vitamin essential for mitochondrial NAD+ -dependent dehydrogenases [pyruvate dehydrogenase and alpha-ketoglutarate dehydrogenase][37]) and the mitochondrial substrate glutamine positively correlated with combination-induced cytotoxicity (Figures 2H, 2I, and S3E), again suggesting that sensitivity to FK866 + reovirus therapy is linked to mitochondrial metabolism. Also supporting a role for energy metabolism, combination-induced production of ADP, an indicator of low-energy status, positively correlated with sensitivity to combination therapy (Figures S3F and S3G). Together, these correlation data support a hypothesis wherein FK866 + reovirus therapy is most effective in MM cells that inherently rely on oxidative phosphorylation over aerobic glycolysis in a p53/KRAS-dependent manner.[33,34] To elucidate the underlying mechanism, we focused on KMS12 cells, as the FK866 + reovirus combination achieved the greatest synergism in this line (Figure S3A).

Reovirus + FK866 combination enhances oncolysis in KMS12 cells independently of reovirus replication

To aid our search for the mechanism facilitating the enhanced sensitivity of KMS12 cells to combination treatment, we comparatively evaluated global proteomes of KMS12 cells untreated or following 24 h of reovirus/NMN/FK866 treatments. We quantified the levels of 5,826 proteins in KMS12 cells (Figure 3A). Principal component analysis (PCA) revealed that reovirus + FK866 induced a protein signature different from monotherapies and controls (Figure 3B). However, the proteins that were altered by combination and reovirus treatments were similar, and the differences between the two groups were subtle (no protein levels were different by more than 2-fold, and enrichment analysis did not reveal any significant differences). In both cases, most proteins that changed were regulated by interferon and were involved in "defense against virus" pathways (Figures S4A–S4D). Examples of proteins increased by reovirus and reovirus + FK866 include OASL, LEG9, IFTI1, IFIT3, ISG15, and OAS2 (Figures S4E–S4J). Furthermore, we did not observe any differences in levels of virus proteins or viral replication at early (12 h.p.i.), mid (24 h.p.i.), or late (48 h.p.i.) replication stages (Figures 3C and 3D). Also, cell surface expression of JAM-A (reovirus receptor), which has previously been reported to correlate with reovirus-induced oncolysis in MM, was not altered by reovirus + FK866 treatment (Figure S4K).[38] Our data thus suggest that increased sensitivity of KMS12 cells to reovirus + FK866 treatment was not caused by early changes in host protein levels or by differences in viral replication.

Reovirus + FK866 combination decreases glucose uptake, glucose flux into TCA cycle, and oxygen consumption in MM cells

To investigate the role of metabolism in enhanced cytotoxicity by reovirus + FK866, we performed global metabolomics analysis in KMS12 cells 24 h post-treatments (Figure 4A). Combination treatment resulted in several unique changes to metabolite levels; for example, reovirus + FK866 increased ADP levels compared with either monotherapy, suggesting decreased energy production (Figure S5A).[39] Also, two TCA cycle intermediates, citrate and malate, were decreased by reovirus + FK866 compared with either monotherapy (Figure 4A), suggesting decreased metabolic flux into mitochondria. As a first approach to determine the mechanism by which combination therapy altered metabolism, we measured glucose uptake 24 h post-reovirus/FK866/NMN treatment. Like the findings from other cancers, reovirus infection alone increased glucose uptake compared with non-infected cells,[14,40–45] whereas reovirus + FK866 reduced glucose uptake

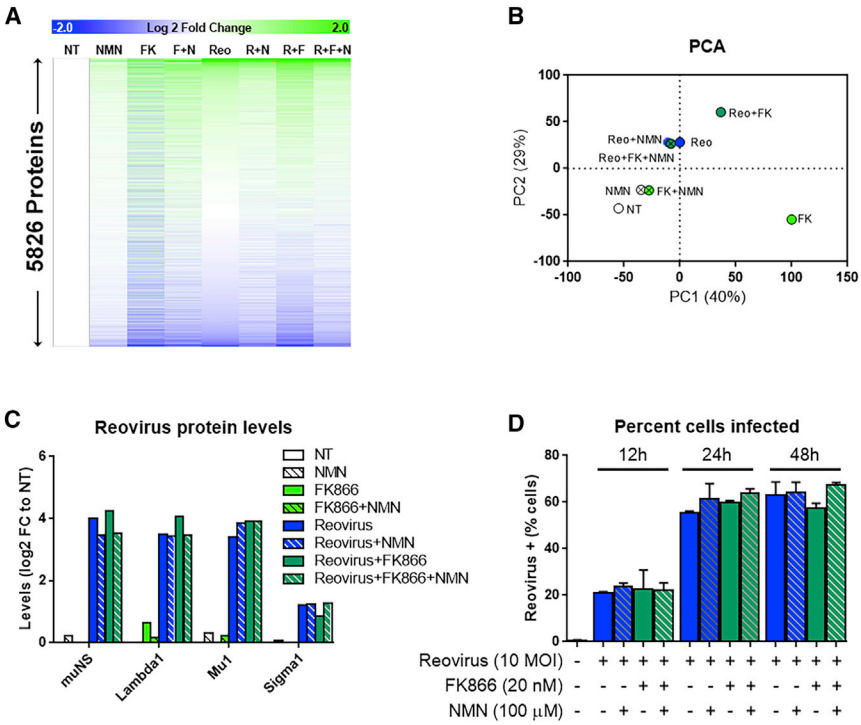

Figure 3. NAMPT inhibition does not enhance reovirus infection or replication in KMS12 cells

(A) Heatmap representing log 2-fold change of 5,826 proteins compared with non-treated (NT) controls by FK866 (20 nM, FK), NMN (100 μM), FK866 + NMN (F + N), reovirus (10 MOI, Reo), reovirus + FK866 (R + F), reovirus and NMN (R + N), or reovirus + FK866 + NMN (R + F + N) 24 h post-treatment. Values represent data from one experiment. (B) PCA of proteomics dataset from (A). (C) Levels of four reovirus proteins extracted from the proteomics data. (D) Percent KMS12 cells infected with reovirus. Data are means ± standard deviation from five independent experiments, each performed in triplicate.

compared with monotherapies and non-treated controls (Figure 4B). To explore the consequences of altered glucose uptake, we conducted untargeted [U-^{13}C]glucose flux analysis beginning 24 h post-treatments. Within 6 h of [U-^{13}C]glucose supplementation, we identified ^{13}C labeling in 35 different metabolites representing a range of pathways including nucleotide, amino acid, and central energy metabolism (Figure S5B). Like other viruses, reovirus infection resulted in a shift of glucose flux toward the pentose phosphate pathway, as was evident by increased ^{13}C labeling of adenine and uracil compared with non-treated controls (Figure S5B).[46–48] One of the largest discrepancies between reovirus + FK866 and monotherapies was flux into the TCA cycle (Figure S5B). Although reovirus alone decreased the flux of [U-^{13}C]glucose into the TCA cycle (as shown by lesser amount of [2-^{13}C]citrate and [2-^{13}C]malate in cells at 6-h post-[U-^{13}C]glucose supplementation), reovirus + FK866 treatment caused a significantly larger drop in 2-^{13}C citrate and malate labeling compared with monotherapies and non-treated control (Figures 4C and S5C). Both reovirus alone and reovirus + FK866 decreased production of [3-^{13}C]lactate from [U-^{13}C]glucose 6 h post-supplementation compared with non-treated controls (Figure S5D). These data suggested that reovirus infection shifted glycolytic flux toward the pentose phosphate pathway, whereas reovirus + FK866 decreased glucose uptake and minimized metabolic flux into the TCA cycle. Supporting our flux analysis, reovirus and combination treatments both decreased extracellular acidification rate (ECAR) and oxygen consumption rate (OCR) compared with non-treated controls, whereas reovirus + FK866 decreased OCR compared with either monotherapy (Figure 4D). Consistent with a reduced glycolytic flux and reduced mitochondrial function, reovirus + FK866 caused a reduction in overall redox capacity compared with monotherapies (Figure 4E). Similar to findings from both monotherapies in other cancer models,[49,50] our data suggest that the reovirus + FK866 combination results in an early synergistic negative effect on central energy metabolism with a drop in mitochondrial function in KMS12 cells (Figure 4F).

Reovirus + FK866 combination induces autophagy-dependent cell death in KMS12 cells

One potential consequence of decreased mitochondrial function is the upregulation of autophagy.[51] Of note, increased autophagic flux has already been linked to both FK866 treatment and reovirus infection in MM cells.[21,52] We found that several autophagy proteins, e.g., Beclin 1, were changed following the treatment with reovirus + FK866 in our proteomics dataset (Figures S6A and S6B). To precisely understand the role of autophagy during reovirus + FK866 combination, we measured autophagic flux by immunoblot analysis of LC3B and STQM1/p62 proteins 24 h after inhibition with chloroquine in KMS12 cells (Figure S6C). As shown (Figures S6D and S6E), the LC3BI-to-LC3BII conversion as well as the levels of p62 were significantly higher following reovirus + FK866 combination compared with monotherapies. These data suggested that reovirus + FK866 treatment promotes autophagic flux in MM cells. To test whether this increase in autophagy contributed to KMS12 cell death following reovirus + FK866 treatment, we measured cell viability in the presence of chloroquine. Supporting the role of autophagy in our model, chloroquine prevented the synergistic effect of combination therapy without affecting the sensitivity to monotherapies (Figure 4G). These data suggest that reovirus + FK866 therapy leads to autophagy-dependent cell death in KMS12 cells.

FK866 potentiates the antitumor efficacy of reovirus-based cancer therapy *in vivo* and reovirus-based oncolysis in patient-derived CD138+ MM cells

To determine the clinical applicability of our findings, we investigated whether the *in vitro* synergistic effect of reovirus + FK866 combination was translatable to *in vivo* contexts. For this purpose, KMS12 tumor-bearing NOD-SCID immunodeficient mice were injected

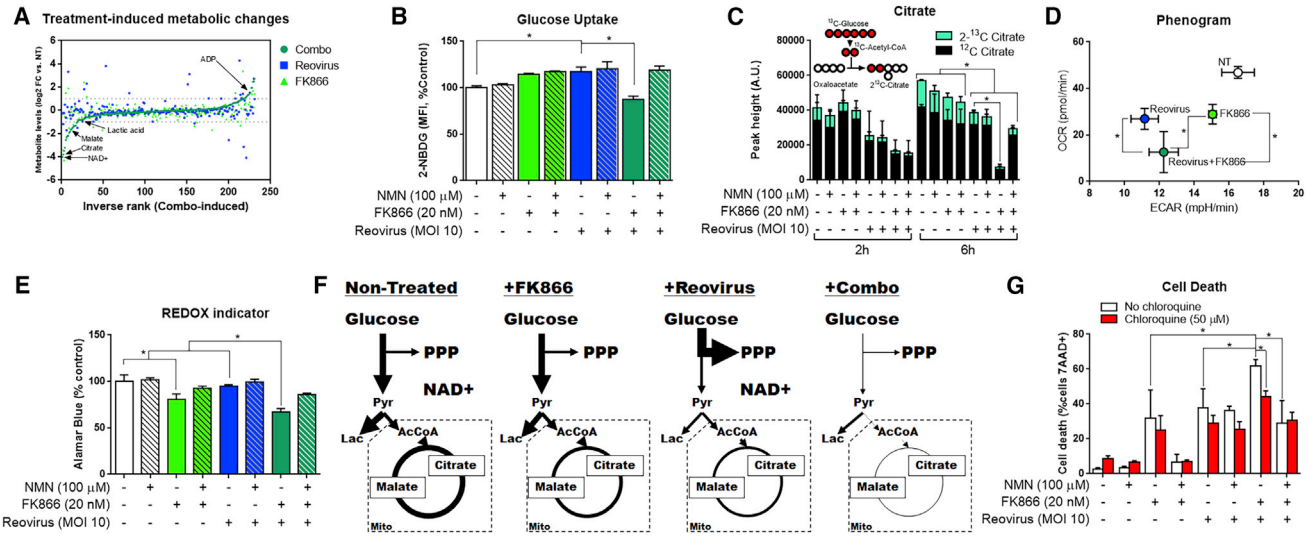

Figure 4. Combination of FK866 + reovirus caused mitochondrial dysfunction in KMS12 cells

(A) Treatment-induced metabolite levels relative to non-treated (NT). (B) Median fluorescent intensity (MFI) of 2-NBDG uptake in 30 min by KMS12 24 h post-treatment. Data are means ± standard deviation from three independent experiments in triplicates. (C) 2-^{13}C-labeled citrate levels 2 and 6 h post [U-^{13}C]glucose supplementation (cells were infected with reovirus and treated with FK866/NMN 24 h before [U-^{13}C]glucose supplementation). Values determined by average peak area of three independent replicates. Indicated statistical significance is for the 2-^{13}C-labeled citrate levels. (D) Oxygen consumption rates (OCR) and extracellular acidification rates (ECAR) measured 24 h post-treatment. Data are means ± standard deviation from three independent wells. Minimal cell death was observed during this time frame. (E) Alamar blue levels of KMS12 cells 24 h post-treatment. Data are means ± standard deviation from three independent experiments in triplicate. (F) Metabolic flux model. Thicker lines represent increased flux. PPP, pentose phosphate pathway; pyr, pyruvate; AcCoA, acetyl-CoA; Lac, lactic acid; mito, mitochondria. (G) Percentage of dead cells 72 h post-treatment. Chloroquine (50 μM) was added at the same time as NMN/FK866/reovirus. Data are means ± standard deviation from three independent experiments in triplicates. *$p < 0.05$.

intratumorally three times with PBS, FK866, and/or reovirus regimens, as shown in Figure 5A. Paralleling our *in vitro* results, tumor-bearing animals treated with the reovirus + FK866 combination showed better survival compared with the tumor-bearing mice treated with either FK866 or reovirus monotherapy or with PBS alone (Figure 5B). Also, tumor volume was generally smaller in KMS12 tumor-bearing mice injected with the combination therapy compared with mice injected with PBS, FK866, or reovirus alone (Figure S7A). These results demonstrated that FK866 enhances the oncolytic efficacy of reovirus in preclinical settings.

Finally, we tested the susceptibility of patient-derived clinical samples to reovirus and/or FK866 (Figures 5C, 5D, and S7B). For this, we propagated cancerous CD138+ and non-cancerous CD138–bone marrow cells from eight MM patients.[53–55] The samples were acquired from patients that ranged from responders to non-responders to standard chemotherapies (Table S2). Only one sample, a non-responder, MM106, contained a loss-of-function mutation in *TP53*; however, other non-responders and partial responders (MM21, MM43, MM57) had a high mutational burden in a wide range of oncogenes, most of which are known to drive aerobic glycolysis (including a frameshift mutation in the p53 activator *ATM*[56] and a missense mutation in *EGR1*, a transcription cofactor that normally facilitates p53-mediated repression of glycolytic genes[36] in MM21; loss-of-function mutations in *FAM46C*, which is normally a repressor of the known aerobic glycolysis activator AKT[57,58] in MM43; V600E mutation in *BRAF*, which causes p53 inactivation,[59] in MM57; gain-of-function mutation in *KRAS* in both MM43 and MM57), whereas very low mutations were detected in the responders (MM44, MM55, and MM67) (Table S3). Of the three responders, only MM55 had two mutations. One, c.5558A > T in *ATM*, has been reported as having no clinical significance,[60,61] while the other, c.1890C > A, is synonymous. Another sample, MM12, only partially responded to chemotherapies but had no detectable mutations. All together, the mutations in the high-mutational-burden samples align with a well-known link between resistance to chemotherapies and high glycolysis/low oxidative phosphorylation in myelomas.[62–68] In accord with a cancer-specific effect of reovirus and FK866, monotherapies and combination therapy had no effect on CD138– cells (Figure S7B). Most importantly, the combination of reovirus + FK866 led to an increase in cytotoxicity and/or a decrease in cell proliferation in CD138+ cells from the low-mutational-burden patient samples (MM12, MM44, MM55, MM67) compared with either of the monotherapies (Figures 5C and 5D). The enhanced cytotoxic effect observed with the reovirus + FK866 combination was abolished upon the addition of NMN (Figures 5C and 5D). The reason that CD138+ cells from the non-responders/high-mutational-burden samples (MM21, MM43, MM57, and MM106) did not respond to combination therapy remains unknown. Nonetheless, it may be linked to an underlying mutational landscape driving aerobic glycolysis (Figures 2C–2I, S3B–S3G; Table S1). Altogether, these data suggest the possibility

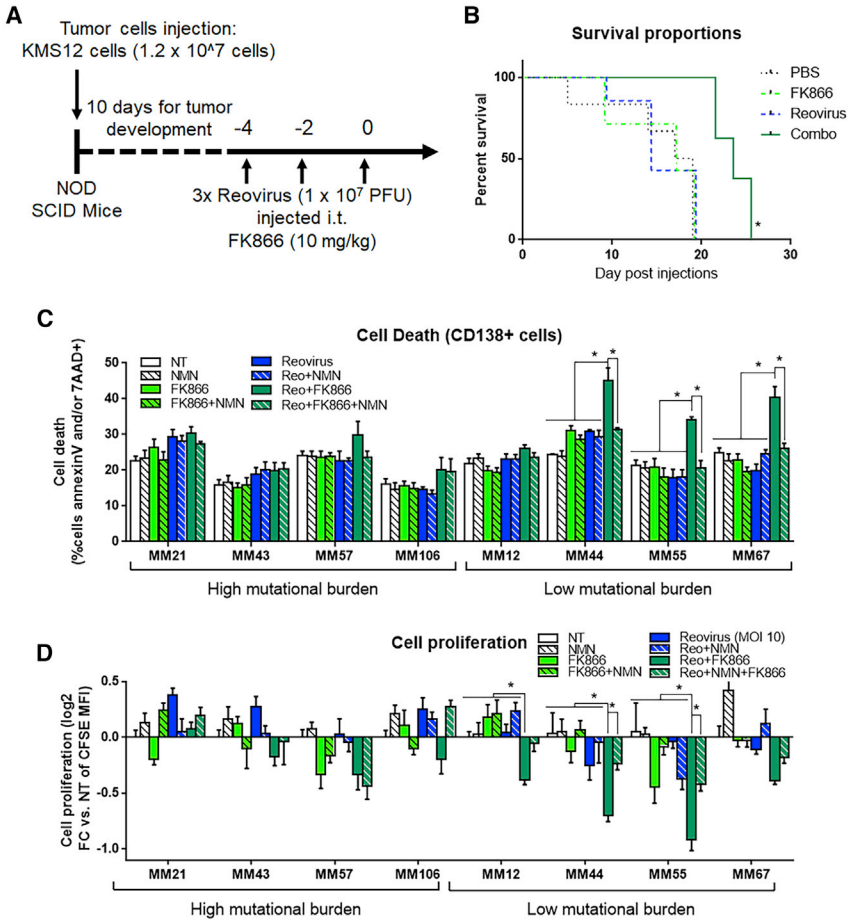

Figure 5. FK866 enhanced antitumor efficacy of reovirus-based cancer therapy *in vivo* and in patient-derived MM samples

(A) Schematic representing the timeline and experimental procedures used during animal experiments. (B) Survival analysis of KMS12 tumor-bearing NOD-SCID mice after three injections of reovirus (1×10^7 PFU), FK866 (10 mg/kg), or a combination of both (Combo). Total mice per treatment: PBS, six mice; FK866, seven mice; reovirus, seven mice; combination, eight mice. (C) Percent cell death as measured by percent annexin V- and/or 7AAD-positive cells 72 h post-treatment in CD138+ patient-derived bone marrow samples. (D) Cell proliferation 120 h post-treatment of CD138+ patient-derived bone marrow samples. Data are means ± standard deviation from three independent experiments, each performed in triplicate. *$p < 0.05$.

of using reovirus + FK866 combination against patient-derived MM cells.

DISCUSSION

Here, we demonstrate how targeting NAD+ synthesis can be used to enhance the efficacy of reovirus-based therapies in MM. Our unbiased metabolomics analysis found that NAD+ levels negatively correlated with oncolytic effects of reovirus in MM (Figures 1C and 1D). We then hypothesized that lowering NAD+ would promote greater sensitivity to reovirus in MM cells. Indeed, we found that the reovirus + FK866 combination promotes significantly higher cytotoxicity in selected MM cell lines, promotes greater survival in MM tumor-bearing animals, and selectively targets patient-derived CD138+ MM cells. Mechanistically, we found that these enhanced cytotoxic effects occur through combination therapy-induced mitochondrial dysfunction promoting autophagy.

There are several documented links between NAD+ and host-pathogen interactions.[69,70] For example, HIV-infected lymphocytes display decreased NAD+ levels,[71] whereas plasmodium-infected erythrocytes and *Leishmania infantum*-infected macrophages show increased NAD+ levels compared with non-infected cells.[72,73] Most of these infection-driven changes in NAD+ levels were mediated through altered NAMPT activity.[72,74,75] Comparable to our findings, group A streptococcus-mediated lysis of human keratinocytes requires a NADase-dependent drop in NAD+ levels and increased autophagic flux (Figures 2B, 2C, 4G, and S6C–S6E).[76,77] The precise connection between NAD+ and pathogen defense in mammalian cells remains unclear. However, in plants, NAD+ protects the host against pathogens through regulation of mitochondrial-generated reactive oxygen species (ROS).[78] Our study suggests a mechanism whereby high NAD+ levels maintain mitochondrial activity in MM cells with functional p53, thus preventing the energy depletion that is required for microbe-driven lysis of the host cell.

NAD+ has been identified as a therapeutic target in MM cells by several studies.[20,21,79–82] Accordingly, we showed that the activity of NAMPT was negatively correlated with the susceptibility of MM cells to reovirus-induced oncolysis (Figure 2A). These data informed our decision to inhibit NAMPT to enhance oncolysis in MM cells. Indeed, FK866 enhanced reovirus oncolysis compared with monotherapies in three of twelve MM cell lines (Figures 2B, 2C, and S3A). We showed that sensitivity to combination therapy positively correlates with expression levels and functionality of p53, which is a known promoter of mitochondrial metabolism and repressor of glycolysis and has previously been shown to be required for both reovirus- and FK866-mediated cytotoxicity (Figures 2C–2E and S3B; Table S1).[25–28] Also, levels of mitochondria-related metabolites and expression of mitochondrial genes all positively correlated with sensitivity to combination therapy, suggesting a role for mitochondria in combination-induced cytotoxicity (Figures 2F–2I and S3D–S3G). In line with our findings, both FK866 and reovirus monotherapies are known to have better responses

in cancers with high mitochondrial function.[12,14,50,83,84] All together, these data suggest that optimal response to reovirus + FK866 combination therapy in MM requires an inherent dependence on mitochondrial metabolism.

We considered various possible mechanisms by which FK866-mediated depletion of NAD+ levels could have enhanced reovirus oncolysis. Although we found no evidence that reovirus infection or replication was altered by combination therapy (Figures 3C and 3D), we did find several indicators of combination therapy-induced mitochondrial dysfunction (Figures 4A–4F), suggesting that the combination of FK866 + reovirus resulted in a synergistic negative effect on mitochondrial function in MM cells. This proposed two-pronged attack on mitochondrial function would potentially overcome the well-documented limitations of FK866 and reovirus as monotherapies.[9,20] As mitochondrial dysfunction promotes autophagy, and it is known that both FK866 and reovirus alone can perturb the autophagic homeostasis in MM cells,[8,21,52] we examined the effect of FK866 + reovirus combination on autophagy. We observed that MM cells treated with FK866 + reovirus displayed higher autophagic flux than that induced by either monotherapy (Figures S6C–S6E). Commonly known as a pro-survival process, autophagy can alternatively lead to cell death under certain circumstances,[85,86] this autophagy-induced cytotoxicity can be prevented by chloroquine.[87–89] Corresponding to autophagic cytotoxicity during combination treatment, we observed that chloroquine prevented cytotoxicity induced by FK866 + reovirus (Figure 4G). Our findings suggest a model wherein the reduction of NAD+ levels through NAMPT inhibition enhances reovirus oncolysis through mitochondrial dysfunction and energy depletion, eventually leading to autophagic cell death.

Our work reveals that the therapeutic inhibition of NAD+ synthesis can be combined with OV to establish an efficacious cancer therapy. It should be noted that, in addition to oncolysis, multiple factors are required for optimal efficacy of OV therapy, including an OV-induced immune response. Although our study shows that NAD+ depletion enhances the oncolytic ability of reovirus, we did not investigate the effect of global NAD+ depletion on other components of the anti-MM response, such as immune cells. In fact, FK866 is known to negatively influence immune cells.[20] Thus, potential therapies involving the combination of NAD+ depletion with OV therapy should further consider possible negative impacts of this combination on OV-induced anti-MM immunity. Nevertheless, considering the already reported therapeutic implications for both NAD+ and reovirus in MM,[8,21,52,79,90] we strongly believe that a combinatorial strategy inhibiting NAD+ synthesis during reovirus therapy promises enhanced anti-MM effects and should be tested in clinical trials.

MATERIALS AND METHODS

Cell lines and reovirus

Reovirus (serotype 3, Dearing strain) was propagated as previously described.[14,91]

Human KMS11, IM9, MM1S, U226, JJN3 (from ATCC), KMM1 (from JCBR), KMS12PE (from Dr. Linda Pilarski [University of Alberta]), and MOLP8, RPMI8226, KMS27, MM1R (from Dr. Jonathan Keats [Translational Genomics Research Institute (TGen)]), and mouse 5TGM1 (from Dr. Babatunde Oyajobi [UT San Antonio]) cell lines were grown and maintained in RPMI 1640 medium supplemented with 10% heat-inactivated FBS, GlutaMAX, sodium pyruvate, non-essential amino acids, and antibiotic-antimycotic.

Animal study

The experimental procedures were governed by the approval of the Ethics Committee at Dalhousie University. Human KMS12 cells were used to generate tumors in 8-week-old female NOD SCID mice (NOD.CB17-Prkdcscid/NCrCrl; Charles River). Visible tumors were injected with a series of three injections (PBS, FK866 [10 mg/kg], and/or reovirus [1×10^7 PFU]), each 2 days apart.

Patient-derived primary multiple myeloma cells

Experimentation on de-identified clinical samples was approved (REB #1024942) by the Nova Scotia Health Authority (NSHA). CD138–and CD138+ cells were cultured in a method adopted from Stockbauer et al.[92] DNA was extracted from purified CD138+ cells positively selected from bone marrow as described previously.[93] DNA mutation analysis was performed and analyzed using a bioinformatic pipeline described previously (additional detail in supplemental methods).[94]

Flow cytometry

Cell death and glucose uptake were determined with 7AAD/annexinV [eBioscience #00-6993-50/#88-8005-74] and 2-NBDG [Thermo #N13195], respectively, as previously described.[14] For reovirus infectivity detection, cancer cells were permeabilized and incubated with a rat anti-reovirus antibody (generated in-house) as previously described.[14] Data acquisition and analysis were completed with BD-FACSCantoII and FCS Express (De Novo), respectively.

Mass spectrometry-based metabolomics

Semi-targeted metabolomics using a data-dependent analysis approach was performed on MM cells. For untargeted metabolic flux analysis, isotopically labeled compounds were identified by comparing labeled and unlabeled samples, using a workflow provided in Compound Discoverer 3.0 (Thermo Scientific). For more information refer to supplemental methods.

Proteomics

Samples were prepared and analyzed (data available, Mendeley Data: https://doi.org/10.17632/7cty2zbz4c.1) with an Orbitrap Fusion mass spectrometer (Thermo Fisher Scientific), using an MS3 method as described previously.[14,95–97] Protein identification was performed as previously described.[14,95]

Metabolic assays

The alamar blue assay was performed according to the manufacturer's instructions (Sigma).[98,99] Oxygen consumption rate (OCR) and extracellular acidification rate (ECAR) by 8×10^4 KMS12 cells

were measured with an XF24 Analyzer according to the manufacturer's protocol for non-adherent cells (Agilent).

Bioinformatics

All mRNA levels were acquired through the CCLE database (data were available from 9 of 12 cell lines; no data for 5TGM1, IM9, or MM1R).[16] *TP53* and *KRAS* mutation status were acquired from the IARC database (http://p53.iarc.fr/).

Statistics

Statistical analysis was done using ANOVA or Kaplan-Meier survival analysis coupled with log rank test (both with 95% confidence interval); p values of <0.05 were considered to be statistically significant. Correlation factors were calculated from datasets that were sampled from Gaussian distribution using Pearson correlation coefficients measuring two-tailed probability. Panther analysis of biological pathways was described previously.[100] For original data, please contact shashi.gujar@dal.ca.

SUPPLEMENTAL INFORMATION

Supplemental information can be found online at https://doi.org/10.1016/j.omto.2022.02.017.

ACKNOWLEDGMENTS

This work was supported by the Dalhousie Medical Research Foundation (DMRF), Canadian Institutes of Health Research (CIHR), Cancer Research Society (CRS), and Beatrice Hunter Cancer Research Institute (BHCRI) to S.G. B.E.K., J.P.M., and M.G. are funded by BHCRI's Cancer Research Training Program (CRTP). B.E.K is also funded by Dalhousie Medical Research Foundation (DMRF)/Infection, Immunity, Inflammation & Vaccinology (I3V). P.K. is funded by Nova Scotia Graduate Scholarship (NSGS). We would like to thank Drs. Alejandro Cohen (Dalhousie University) and Sylvere Durand (Gustave Roussy) for their expertise with metabolomics and mass spectrometry. The graphical abstract was created with BioRender.com. Finally, we thank the Dalhousie University animal care facility and staff for general maintenance of all animals used in this study.

AUTHOR CONTRIBUTIONS

Conception and design: B.E. Kennedy and S. Gujar. Development of methodology: B.E. Kennedy, M. Giacomantonio, J.P. Murphy, S. Cutler, P. Konda, S. Cutler, J.A. Paulo, and D. Gaston. Acquisition of data (provided animals, acquired and managed patients, provided facilities, etc.): B.E. Kennedy, M. Giacomantonio, J.P. Murphy, S. Cutler, M. Sadek, J.A. Paulo, G.P. Pathak, S. Renkens, S. Grieve, A. Cohen, J. Pol, G. Kroemer, S.P. Gygi, C. Richardson, M.O. Elnenaei, D. Gaston, T. Reiman, and S. Gujar. Analysis and interpretation of data (e.g., statistical analysis, biostatistics, computational analysis): B.E. Kennedy, J.P. Murphy, P. Konda, M. Giacomantonio, S. Cutler, and J.A. Paulo. Writing, review, and/or revision of the manuscript: B.E. Kennedy, J.P. Murphy, M. Giacomantonio, S. Cutler, M. Sadek, and S. Gujar. Administrative, technical, or material support (i.e., reporting or organizing data, constructing databases): B.E. Kennedy, J.P. Murphy, and S. Gujar. Study supervision: S. Gujar. Other (funding): S. Gujar.

DECLARATION OF INTEREST

The authors declare that they have no conflict of interest or competing financial interests.

REFERENCES

1. Rajkumar, S.V., Dimopoulos, M.A., Palumbo, A., Blade, J., Merlini, G., Mateos, M.V., Kumar, S., Hillengass, J., Kastritis, E., Richardson, P., et al. (2014). International Myeloma Working Group updated criteria for the diagnosis of multiple myeloma. Lancet Oncol. *15*, 538–548.
2. Siegel, R., Ma, J., Zou, Z., and Jemal, A. (2014). Cancer statistics, 2014. CA Cancer J. Clin. *64*, 9–29.
3. Thirukkumaran, C.M., and Morris, D.G. (2011). Oncolytic virotherapy for multiple myeloma: past, present, and future. Bone Marrow Res. *2011*, 632948.
4. Lawler, S.E., Speranza, M.C., Cho, C.F., and Chiocca, E.A. (2017). Oncolytic viruses in cancer treatment: a review. JAMA Oncol. *3*, 841–849.
5. Fountzilas, C., Patel, S., and Mahalingam, D. (2017). Review: oncolytic virotherapy, updates and future directions. Oncotarget *8*, 102617–102639.
6. Coffey, M.C., Strong, J.E., Forsyth, P.A., and Lee, P.W. (1998). Reovirus therapy of tumors with activated Ras pathway. Science *282*, 1332–1334.
7. Kelly, K.R., Espitia, C.M., Mahalingam, D., Oyajobi, B.O., Coffey, M., Giles, F.J., Carew, J.S., and Nawrocki, S.T. (2012). Reovirus therapy stimulates endoplasmic reticular stress, NOXA induction, and augments bortezomib-mediated apoptosis in multiple myeloma. Oncogene *31*, 3023–3038.
8. Thirukkumaran, C.M., Shi, Z.Q., Luider, J., Kopciuk, K., Gao, H., Bahlis, N., Neri, P., Pho, M., Stewart, D., Mansoor, A., et al. (2012). Reovirus as a viable therapeutic option for the treatment of multiple myeloma. Clin. Cancer Res. *18*, 4962–4972.
9. Sborov, D.W., Nuovo, G.J., Stiff, A., Mace, T., Lesinski, G.B., Benson, D.M., Jr., Efebera, Y.A., Rosko, A.E., Pichiorri, F., Grever, M.R., et al. (2014). A phase I trial of single-agent reolysin in patients with relapsed multiple myeloma. Clin. Cancer Res. *20*, 5946–5955.
10. Stiff, A., Caserta, E., Sborov, D.W., Nuovo, G.J., Mo, X., Schlotter, S.Y., Canella, A., Smith, E., Badway, J., Old, M., et al. (2016). Histone deacetylase inhibitors enhance the therapeutic potential of reovirus in multiple myeloma. Mol. Cancer Ther. *15*, 830–841.
11. Thirukkumaran, C.M., Shi, Z.Q., Nuovo, G.J., Luider, J., Kopciuk, K.A., Dong, Y., Mostafa, A.A., Thakur, S., Gratton, K., Yang, A., et al. (2019). Oncolytic immunotherapy and bortezomib synergy improves survival of refractory multiple myeloma in a preclinical model. Blood Adv. *3*, 797–812.
12. Kennedy, B.E., Sadek, M., and Gujar, S.A. (2020). Targeted metabolic reprogramming to improve the efficacy of oncolytic virus therapy. Mol. Ther. *28*, 1417–1421.
13. Thaker, S.K., Ch'ng, J., and Christofk, H.R. (2019). Viral hijacking of cellular metabolism. BMC Biol. *17*, 59.
14. Kennedy, B.E., Murphy, J.P., Clements, D.R., Konda, P., Holay, N., Kim, Y., Pathak, G.P., Giacomantonio, M.A., Hiani, Y.E., and Gujar, S. (2019). Inhibition of pyruvate dehydrogenase kinase enhances the antitumor efficacy of oncolytic reovirus. Cancer Res. *79*, 3824–3836.
15. Rizzieri, D., Paul, B., and Kang, Y. (2019). Metabolic alterations and the potential for targeting metabolic pathways in the treatment of multiple myeloma. J. Cancer Metastasis Treat. *5*, 26.
16. Ghosh, D., Levault, K.R., and Brewer, G.J. (2014). Relative importance of redox buffers GSH and NAD(P)H in age-related neurodegeneration and Alzheimer disease-like mouse neurons. Aging Cell *13*, 631–640.
17. Tan, B., Young, D.A., Lu, Z.H., Wang, T., Meier, T.I., Shepard, R.L., Roth, K., Zhai, Y., Huss, K., Kuo, M.S., et al. (2013). Pharmacological inhibition of nicotinamide phosphoribosyltransferase (NAMPT), an enzyme essential for NAD+ biosynthesis, in human cancer cells: metabolic basis and potential clinical implications. J. Biol. Chem. *288*, 3500–3511.

18. Zhou, X., Curbo, S., Li, F., Krishnan, S., and Karlsson, A. (2018). Inhibition of glutamate oxaloacetate transaminase 1 in cancer cell lines results in altered metabolism with increased dependency of glucose. BMC Cancer *18*, 559.

19. Barretina, J., Caponigro, G., Stransky, N., Venkatesan, K., Margolin, A.A., Kim, S., Wilson, C.J., Lehar, J., Kryukov, G.V., Sonkin, D., et al. (2012). The Cancer Cell Line Encyclopedia enables predictive modelling of anticancer drug sensitivity. Nature *483*, 603–607.

20. Kennedy, B.E., Sharif, T., Martell, E., Dai, C., Kim, Y., Lee, P.W., and Gujar, S.A. (2016). NAD(+) salvage pathway in cancer metabolism and therapy. Pharmacol. Res. *114*, 274–283.

21. Cea, M., Cagnetta, A., Fulciniti, M., Tai, Y.T., Hideshima, T., Chauhan, D., Roccaro, A., Sacco, A., Calimeri, T., Cottini, F., et al. (2012). Targeting NAD+ salvage pathway induces autophagy in multiple myeloma cells via mTORC1 and extracellular signal-regulated kinase (ERK1/2) inhibition. Blood *120*, 3519–3529.

22. Meyers, R.M., Bryan, J.G., McFarland, J.M., Weir, B.A., Sizemore, A.E., Xu, H., Dharia, N.V., Montgomery, P.G., Cowley, G.S., Pantel, S., et al. (2017). Computational correction of copy number effect improves specificity of CRISPR-Cas9 essentiality screens in cancer cells. Nat. Genet. *49*, 1779–1784.

23. Penke, M., Schuster, S., Gorski, T., Gebhardt, R., Kiess, W., and Garten, A. (2017). Oleate ameliorates palmitate-induced reduction of NAMPT activity and NAD levels in primary human hepatocytes and hepatocarcinoma cells. Lipids Health Dis. *16*, 191.

24. Hasmann, M., and Schemainda, I. (2003). FK866, a highly specific noncompetitive inhibitor of nicotinamide phosphoribosyltransferase, represents a novel mechanism for induction of tumor cell apoptosis. Cancer Res. *63*, 7436–7442.

25. Thakur, B.K., Dittrich, T., Chandra, P., Becker, A., Kuehnau, W., Klusmann, J.H., Reinhardt, D., and Welte, K. (2013). Involvement of p53 in the cytotoxic activity of the NAMPT inhibitor FK866 in myeloid leukemic cells. Int. J. Cancer *132*, 766–774.

26. Pan, D., Marcato, P., Ahn, D.G., Gujar, S., Pan, L.Z., Shmulevitz, M., and Lee, P.W. (2013). Activation of p53 by chemotherapeutic agents enhances reovirus oncolysis. PLoS One *8*, e54006.

27. Pan, D., Pan, L.Z., Hill, R., Marcato, P., Shmulevitz, M., Vassilev, L.T., and Lee, P.W. (2011). Stabilisation of p53 enhances reovirus-induced apoptosis and virus spread through p53-dependent NF-kappaB activation. Br. J. Cancer *105*, 1012–1022.

28. Zhang, X., Wu, H., Liu, C., Tian, J., and Qu, L. (2015). PI3K/Akt/p53 pathway inhibits reovirus infection. Infect. Genet. Evol. *34*, 415–422.

29. Giacomelli, A.O., Yang, X., Lintner, R.E., McFarland, J.M., Duby, M., Kim, J., Howard, T.P., Takeda, D.Y., Ly, S.H., Kim, E., et al. (2018). Mutational processes shape the landscape of TP53 mutations in human cancer. Nat. Genet. *50*, 1381–1387.

30. Davison, T.S., Yin, P., Nie, E., Kay, C., and Arrowsmith, C.H. (1998). Characterization of the oligomerization defects of two p53 mutants found in families with Li-Fraumeni and Li-Fraumeni-like syndrome. Oncogene *17*, 651–656.

31. Zhao, Y., Chen, X.Q., and Du, J.Z. (2009). Cellular adaptation to hypoxia and p53 transcription regulation. J. Zhejiang Univ. Sci. B *10*, 404–410.

32. Mancini, F., Gentiletti, F., D'Angelo, M., Giglio, S., Nanni, S., D'Angelo, C., Farsetti, A., Citro, G., Sacchi, A., Pontecorvi, A., et al. (2004). MDM4 (MDMX) overexpression enhances stabilization of stress-induced p53 and promotes apoptosis. J. Biol. Chem. *279*, 8169–8180.

33. Kawada, K., Toda, K., and Sakai, Y. (2017). Targeting metabolic reprogramming in KRAS-driven cancers. Int. J. Clin. Oncol. *22*, 651–659.

34. Puzio-Kuter, A.M. (2011). The role of p53 in metabolic regulation. Genes Cancer *2*, 385–391.

35. Wang, J., Zhang, P., Zhong, J., Tan, M., Ge, J., Tao, L., Li, Y., Zhu, Y., Wu, L., Qiu, J., et al. (2016). The platelet isoform of phosphofructokinase contributes to metabolic reprogramming and maintains cell proliferation in clear cell renal cell carcinoma. Oncotarget *7*, 27142–27157.

36. Zawacka-Pankau, J., Grinkevich, V.V., Hunten, S., Nikulenkov, F., Gluch, A., Li, H., Enge, M., Kel, A., and Selivanova, G. (2011). Inhibition of glycolytic enzymes mediated by pharmacologically activated p53: targeting Warburg effect to fight cancer. J. Biol. Chem. *286*, 41600–41615.

37. Mkrtchyan, G.V., Ucal, M., Mullebner, A., Dumitrescu, S., Kames, M., Moldzio, R., Molcanyi, M., Schaefer, S., Weidinger, A., Schaefer, U., et al. (2018). Thiamine preserves mitochondrial function in a rat model of traumatic brain injury, preventing inactivation of the 2-oxoglutarate dehydrogenase complex. Biochim. Biophys. Acta Bioenerg. *1859*, 925–931.

38. Kelly, K.R., Espitia, C.M., Zhao, W., Wendlandt, E., Tricot, G., Zhan, F., Carew, J.S., and Nawrocki, S.T. (2015). Junctional adhesion molecule-A is overexpressed in advanced multiple myeloma and determines response to oncolytic reovirus. Oncotarget *6*, 41275–41289.

39. Hardie, D.G. (2003). Minireview: the AMP-activated protein kinase cascade: the key sensor of cellular energy status. Endocrinology *144*, 5179–5183.

40. Singh, V.N., Singh, M., August, J.T., and Horecker, B.L. (1974). Alterations in glucose metabolism in chick-embryo cells transformed by Rous sarcoma virus: intracellular levels of glycolytic intermediates. Proc. Natl. Acad. Sci. U S A *71*, 4129–4132.

41. Green, M., Henle, G., and Deinhardt, F. (1958). Respiration and glycolysis of human cells grown in tissue culture. Virology *5*, 206–219.

42. Landini, M.P. (1984). Early enhanced glucose uptake in human cytomegalovirus-infected cells. J. Gen. Virol. *65* (Pt 7), 1229–1232.

43. Klemperer, H. (1961). Glucose breakdown in chick embryo cells infected with influenza virus. Virology *13*, 68–77.

44. Levy, H.B., and Baron, S. (1957). The effect of animal viruses on host cell metabolism. II. Effect of poliomyelitis virus on glycolysis and uptake of glycine by monkey kidney tissue cultures. J. Infect. Dis. *100*, 109–118.

45. Bardell, D., and Essex, M. (1974). Glycolysis during early infection of feline and human cells with feline leukemia virus. Infect. Immun. *9*, 824–827.

46. Thai, M., Graham, N.A., Braas, D., Nehil, M., Komisopoulou, E., Kurdistani, S.K., McCormick, F., Graeber, T.G., and Christofk, H.R. (2014). Adenovirus E4ORF1-induced MYC activation promotes host cell anabolic glucose metabolism and virus replication. Cell Metab. *19*, 694–701.

47. Munger, J., Bajad, S.U., Coller, H.A., Shenk, T., and Rabinowitz, J.D. (2006). Dynamics of the cellular metabolome during human cytomegalovirus infection. PLoS Pathog. *2*, e132.

48. Jung, G.S., Jeon, J.H., Choi, Y.K., Jang, S.Y., Park, S.Y., Kim, S.W., Byun, J.K., Kim, M.K., Lee, S., Shin, E.C., et al. (2016). Pyruvate dehydrogenase kinase regulates hepatitis C virus replication. Sci. Rep. *6*, 30846.

49. Clarke, P., Richardson-Burns, S.M., DeBiasi, R.L., and Tyler, K.L. (2005). Mechanisms of apoptosis during reovirus infection. Curr. Top. Microbiol. Immunol. *289*, 1–24.

50. Oyarzun, A.P., Westermeier, F., Pennanen, C., Lopez-Crisosto, C., Parra, V., Sotomayor-Flores, C., Sanchez, G., Pedrozo, Z., Troncoso, R., and Lavandero, S. (2015). FK866 compromises mitochondrial metabolism and adaptive stress responses in cultured cardiomyocytes. Biochem. Pharmacol. *98*, 92–101.

51. Rabinowitz, J.D., and White, E. (2010). Autophagy and metabolism. Science *330*, 1344–1348.

52. Thirukkumaran, C.M., Shi, Z.Q., Luider, J., Kopciuk, K., Gao, H., Bahlis, N., Neri, P., Pho, M., Stewart, D., Mansoor, A., et al. (2013). Reovirus modulates autophagy during oncolysis of multiple myeloma. Autophagy *9*, 413–414.

53. Khotskaya, Y.B., Dai, Y., Ritchie, J.P., MacLeod, V., Yang, Y., Zinn, K., and Sanderson, R.D. (2009). Syndecan-1 is required for robust growth, vascularization, and metastasis of myeloma tumors *in vivo*. J. Biol. Chem. *284*, 26085–26095.

54. O'Connell, F.P., Pinkus, J.L., and Pinkus, G.S. (2004). CD138 (syndecan-1), a plasma cell marker immunohistochemical profile in hematopoietic and nonhematopoietic neoplasms. Am. J. Clin. Pathol. *121*, 254–263.

55. Yang, Y., MacLeod, V., Dai, Y., Khotskaya-Sample, Y., Shriver, Z., Venkataraman, G., Sasisekharan, R., Naggi, A., Torri, G., Casu, B., et al. (2007). The syndecan-1 heparan sulfate proteoglycan is a viable target for myeloma therapy. Blood *110*, 2041–2048.

56. Turenne, G.A., Paul, P., Laflair, L., and Price, B.D. (2001). Activation of p53 transcriptional activity requires ATM's kinase domain and multiple N-terminal serine residues of p53. Oncogene *20*, 5100–5110.

57. Kanasugi, J., Hanamura, I., Ota, A., Karnan, S., Lam, V.Q., Mizuno, S., Wahiduzzaman, M., Rahman, M.L., Hyodo, T., Konishi, H., et al. (2020). Biallelic loss of FAM46C triggers tumor growth with concomitant activation of Akt signaling in multiple myeloma cells. Cancer Sci. *111*, 1663–1675.

58. Elstrom, R.L., Bauer, D.E., Buzzai, M., Karnauskas, R., Harris, M.H., Plas, D.R., Zhuang, H., Cinalli, R.M., Alavi, A., Rudin, C.M., et al. (2004). Akt stimulates aerobic glycolysis in cancer cells. Cancer Res. *64*, 3892–3899.

59. Yu, H., McDaid, R., Lee, J., Possik, P., Li, L., Kumar, S.M., Elder, D.E., Van Belle, P., Gimotty, P., Guerra, M., et al. (2009). The role of BRAF mutation and p53 inactivation during transformation of a subpopulation of primary human melanocytes. Am. J. Pathol. *174*, 2367–2377.

60. Nykamp, K., Anderson, M., Powers, M., Garcia, J., Herrera, B., Ho, Y.Y., Kobayashi, Y., Patil, N., Thusberg, J., Westbrook, M., et al. (2017). Sherloc: a comprehensive refinement of the ACMG-AMP variant classification criteria. Genet. Med. *19*, 1105–1117.

61. Sandoval, N., Platzer, M., Rosenthal, A., Dork, T., Bendix, R., Skawran, B., Stuhrmann, M., Wegner, R.D., Sperling, K., Banin, S., et al. (1999). Characterization of ATM gene mutations in 66 ataxia telangiectasia families. Hum. Mol. Genet. *8*, 69–79.

62. Friday, E., Ledet, J., and Turturro, F. (2011). Response to dexamethasone is glucose-sensitive in multiple myeloma cell lines. J. Exp. Clin. Cancer Res. *30*, 81.

63. Yu, W., Cao, D., Zhou, H., Hu, Y., and Guo, T. (2015). PGC-1alpha is responsible for survival of multiple myeloma cells under hyperglycemia and chemotherapy. Oncol. Rep. *33*, 2086–2092.

64. McBrayer, S.K., Cheng, J.C., Singhal, S., Krett, N.L., Rosen, S.T., and Shanmugam, M. (2012). Multiple myeloma exhibits novel dependence on GLUT4, GLUT8, and GLUT11: implications for glucose transporter-directed therapy. Blood *119*, 4686–4697.

65. Zaal, E.A., Wu, W., Jansen, G., Zweegman, S., Cloos, J., and Berkers, C.R. (2017). Bortezomib resistance in multiple myeloma is associated with increased serine synthesis. Cancer Metab. *5*, 7.

66. Maiso, P., Huynh, D., Moschetta, M., Sacco, A., Aljawai, Y., Mishima, Y., Asara, J.M., Roccaro, A.M., Kimmelman, A.C., and Ghobrial, I.M. (2015). Metabolic signature identifies novel targets for drug resistance in multiple myeloma. Cancer Res. *75*, 2071–2082.

67. Sanchez, W.Y., McGee, S.L., Connor, T., Mottram, B., Wilkinson, A., Whitehead, J.P., Vuckovic, S., and Catley, L. (2013). Dichloroacetate inhibits aerobic glycolysis in multiple myeloma cells and increases sensitivity to bortezomib. Br. J. Cancer *108*, 1624–1633.

68. Zaal, E.A., and Berkers, C.R. (2018). The influence of metabolism on drug response in cancer. Front. Oncol. *8*, 500.

69. Mesquita, I., Varela, P., Belinha, A., Gaifem, J., Laforge, M., Vergnes, B., Estaquier, J., and Silvestre, R. (2016). Exploring NAD+ metabolism in host-pathogen interactions. Cell Mol. Life Sci. *73*, 1225–1236.

70. Domergue, R., Castano, I., De Las Penas, A., Zupancic, M., Lockatell, V., Hebel, J.R., Johnson, D., and Cormack, B.P. (2005). Nicotinic acid limitation regulates silencing of Candida adhesins during UTI. Science *308*, 866–870.

71. Murray, M.F., Nghiem, M., and Srinivasan, A. (1995). HIV infection decreases intracellular nicotinamide adenine dinucleotide [NAD]. Biochem. Biophys. Res. Commun. *212*, 126–131.

72. Zerez, C.R., Roth, E.F., Jr., Schulman, S., and Tanaka, K.R. (1990). Increased nicotinamide adenine dinucleotide content and synthesis in Plasmodium falciparum-infected human erythrocytes. Blood *75*, 1705–1710.

73. Moreira, D., Rodrigues, V., Abengozar, M., Rivas, L., Rial, E., Laforge, M., Li, X., Foretz, M., Viollet, B., Estaquier, J., et al. (2015). Leishmania infantum modulates host macrophage mitochondrial metabolism by hijacking the SIRT1-AMPK axis. PLoS Pathog. *11*, e1004684.

74. Chen, X.Y., Zhang, H.S., Wu, T.C., Sang, W.W., and Ruan, Z. (2013). Down-regulation of NAMPT expression by miR-182 is involved in Tat-induced HIV-1 long terminal repeat (LTR) transactivation. Int. J. Biochem. Cell Biol. *45*, 292–298.

75. Dantoft, W., Robertson, K.A., Watkins, W.J., Strobl, B., and Ghazal, P. (2019). Metabolic regulators Nampt and Sirt6 serially participate in the macrophage interferon antiviral cascade. Front. Microbiol. *10*, 355.

76. Michos, A., Gryllos, I., Hakansson, A., Srivastava, A., Kokkotou, E., and Wessels, M.R. (2006). Enhancement of streptolysin O activity and intrinsic cytotoxic effects of the group A streptococcal toxin, NAD-glycohydrolase. J. Biol. Chem. *281*, 8216–8223.

77. O'Seaghdha, M., and Wessels, M.R. (2013). Streptolysin O and its co-toxin NAD-glycohydrolase protect group A Streptococcus from Xenophagic killing. PLoS Pathog. *9*, e1003394.

78. Hashida, S.N., Takahashi, H., and Uchimiya, H. (2009). The role of NAD biosynthesis in plant development and stress responses. Ann. Bot. *103*, 819–824.

79. Cea, M., Cagnetta, A., Patrone, F., Nencioni, A., Gobbi, M., and Anderson, K.C. (2013). Intracellular NAD(+) depletion induces autophagic death in multiple myeloma cells. Autophagy *9*, 410–412.

80. Cea, M., Cagnetta, A., Adamia, S., Acharya, C., Tai, Y.T., Fulciniti, M., Ohguchi, H., Munshi, A., Acharya, P., Bhasin, M.K., et al. (2016). Evidence for a role of the histone deacetylase SIRT6 in DNA damage response of multiple myeloma cells. Blood *127*, 1138–1150.

81. Cagnetta, A., Cea, M., Calimeri, T., Acharya, C., Fulciniti, M., Tai, Y.T., Hideshima, T., Chauhan, D., Zhong, M.Y., Patrone, F., et al. (2013). Intracellular NAD(+) depletion enhances bortezomib-induced anti-myeloma activity. Blood *122*, 1243–1255.

82. Kennedy, B.E., Sadek, M., Elnenaei, M.O., Reiman, A., and Gujar, S.A. (2020). Targeting NAD(+) synthesis to potentiate CD38-based immunotherapy of multiple myeloma. Trends Cancer *6*, 9–12.

83. Xu, R., Yuan, Z., Yang, L., Li, L., Li, D., and Lv, C. (2017). Inhibition of NAMPT decreases cell growth and enhances susceptibility to oxidative stress. Oncol. Rep. *38*, 1767–1773.

84. Thongon, N., Zucal, C., D'Agostino, V.G., Tebaldi, T., Ravera, S., Zamporlini, F., Piacente, F., Moschoi, R., Raffaelli, N., Quattrone, A., et al. (2018). Cancer cell metabolic plasticity allows resistance to NAMPT inhibition but invariably induces dependence on LDHA. Cancer Metab. *6*, 1.

85. Yonekawa, T., and Thorburn, A. (2013). Autophagy and cell death. Essays Biochem. *55*, 105–117.

86. Shimizu, S., Yoshida, T., Tsujioka, M., and Arakawa, S. (2014). Autophagic cell death and cancer. Int. J. Mol. Sci. *15*, 3145–3153.

87. Xu, L., and Wang, Z. (2016). Chloroquine rescues A549 cells from paraquat-induced death. Drug Chem. Toxicol. *39*, 167–173.

88. Park, D., and Lee, Y. (2014). Biphasic activity of chloroquine in human colorectal cancer cells. Dev. Reprod. *18*, 225–231.

89. Hirata, Y., Yamamoto, H., Atta, M.S., Mahmoud, S., Oh-hashi, K., and Kiuchi, K. (2011). Chloroquine inhibits glutamate-induced death of a neuronal cell line by reducing reactive oxygen species through sigma-1 receptor. J. Neurochem. *119*, 839–847.

90. Kelly, K.R., Espitia, C.M., Zhao, W., Wu, K., Visconte, V., Anwer, F., Calton, C.M., Carew, J.S., and Nawrocki, S.T. (2018). Oncolytic reovirus sensitizes multiple myeloma cells to anti-PD-L1 therapy. Leukemia *32*, 230–233.

91. Smith, R.E., Zweerink, H.J., and Joklik, W.K. (1969). Polypeptide components of virions, top component and cores of reovirus type 3. Virology *39*, 791–810.

92. Stockbauer, P., Spicka, I., Otevrelova, P., Straub, J., Hradcova, M., and Klener, P. (2002). [Long-term culture of plasma cells from patients with myeloma and establishment of a permanent cell line]. Sb Lek *103*, 371–377.

93. Elnenaei, M.O., Knopf, P., Cutler, S.D., Sinclair, K., Abou El Hassan, M., Greer, W., Goudie, M., Wagner, J., White, D., Couban, S., et al. (2019). Low-depth sequencing for copy number abnormalities in multiple myeloma supersedes fluorescent *in situ* hybridization in scope and resolution. Clin. Genet. *96*, 163–168.

94. Carter, M.D., Gaston, D., Huang, W.Y., Greer, W.L., Pasternak, S., Ly, T.Y., and Walsh, N.M. (2018). Genetic profiles of different subsets of Merkel cell carcinoma show links between combined and pure MCPyV-negative tumors. Hum. Pathol. *71*, 117–125.

95. Murphy, J.P., Stepanova, E., Everley, R.A., Paulo, J.A., and Gygi, S.P. (2015). Comprehensive temporal protein dynamics during the diauxic shift in Saccharomyces cerevisiae. Mol. Cell. Proteomics *14*, 2454–2465.

96. Rappsilber, J., Ishihama, Y., and Mann, M. (2003). Stop and go extraction tips for matrix-assisted laser desorption/ionization, nanoelectrospray, and LC/MS sample pretreatment in proteomics. Anal. Chem. *75*, 663–670.

97. Ting, L., Rad, R., Gygi, S.P., and Haas, W. (2011). MS3 eliminates ratio distortion in isobaric multiplexed quantitative proteomics. Nat. Methods *8*, 937–940.

98. O'Brien, J., Wilson, I., Orton, T., and Pognan, F. (2000). Investigation of the Alamar Blue (resazurin) fluorescent dye for the assessment of mammalian cell cytotoxicity. Eur. J. Biochem. *267*, 5421–5426.

99. Rampersad, S.N. (2012). Multiple applications of Alamar Blue as an indicator of metabolic function and cellular health in cell viability bioassays. Sensors (Basel) *12*, 12347–12360.

100. Mi, H., Muruganujan, A., Ebert, D., Huang, X., and Thomas, P.D. (2019). PANTHER version 14: more genomes, a new PANTHER GO-slim and improvements in enrichment analysis tools. Nucleic Acids Res. *47*, D419–D426.